Supplementary Materials for

"Characterization of Blood Flow in the Mouse Dorsal Spinal Venous System Before and After Dorsal Spinal Vein Occlusion"

Two-parameter dAV fitting model

We assumed Poiseuille flow given by Equation (3). We further assumed the resistance to be a composite resistance given by Equation (6). The radius-dependent resistance is given by Equation (4). Combining these equations, we find:

$$Q(r) = \frac{\Delta P}{R_{UBV} + \left(\frac{8\eta L}{\pi r^4}\right)} \quad \text{(S1)}$$

We assumed that for dAVs in close proximity to each other, the pressure difference across each dAV could be taken to be approximately equal because there is little change in pressure along the dSV between closely spaced dAVs. In this case, Equation (S1) reduces to a two-parameter model given by:

$$Q(r) = \frac{a}{1 + br^{-4}} \quad \text{(S2)}$$

where

$$a = \frac{\Delta P}{R_{UBV}} \quad \text{(S3)}$$

and

$$b = \frac{8\eta L}{\pi R_{UBV}} \quad \text{(S4)}$$

Network model of dorsal SCBF with fixed resistances

We considered a network model of 100 dAVs of resistance R_0 joined to segments of the dSV. Given that the mean dAV diameter was approximately 25 μm and the mean dSV diameter was approximately 140 μm, we used Equation (6) to estimate

$$R_{dSV} = \left(\frac{25}{140}\right)^4 R_0 \approx 10^{-3} R_0 \quad \text{(S5)}$$

We further assumed that each dAV had a distal pressure source of P_0 and took the exiting branches from the dSV as our zero-pressure reference point. For book-keeping purposes, we labeled the dAVs by even indices and the dSV segments by odd indices in our flow matrix, such that vessel j had resistance R_j given by

$$R_j = \begin{cases} R_0, j \text{ even} \\ R_{dSV}, j \text{ odd} \end{cases} \quad \text{(S6)}$$

The flow matrix can then be constructed by conservation of flow at each junction of two dSV segments and one dAV as:

$$Q_{2j+1} = Q_{2j} + Q_{2j-1}, j = 1,2, \dots N \quad \text{(S7)}$$

and by summing pressure drops using Equation (3):

$$P_0 - Q_{2j} R_0 - 10^{-3} R_0 \sum_{n=1}^{j} Q_{2n-1} = 0 \quad \text{(S8)}$$

By defining the unit of flow such that:

$$\frac{P_0}{R_0} \equiv 1 \quad \text{(S9)}$$

Equation (S8) then becomes

$$1 - Q_{2j} - 10^{-3} \sum_{n=1}^{j} Q_{2n-1} = 0 \quad \text{(S10)}$$

Equations (S7) and (S10) define a dimensionless flow matrix, which can be solved numerically to give the flows in the dAVs and dSV segments by reducing to row-reduced echelon form.

To simulate a clot in the dSV just above the j^{th} dAV, we let:

$$R_{2j+1} \to 10^4 R_0 \qquad \text{(S11)}$$

And solved the flow matrix as before by reducing to row-reduced echelon form. Due to numerical limitations, it was necessary to use a large value for the resistance rather than a truly infinite value as might be assumed in theory.

Network model of dorsal SCBF with variable resistances

To test how variation in dAV resistance would affect our model, we generated 100 dAVs with radii taken from a normal distribution of mean 25 μm and standard deviation of 10 μm in accordance with our *in vivo* observations. The subsequent resistances were given by Equation (5). In this case, Equation (S10) has the form:

$$1 - \left(\frac{12.5\ \mu\text{m}}{r_j}\right)^4 Q_{2j} - 10^{-3} \sum_{n=1}^{j} Q_{2n-1} = 0 \qquad \text{(S12)}$$

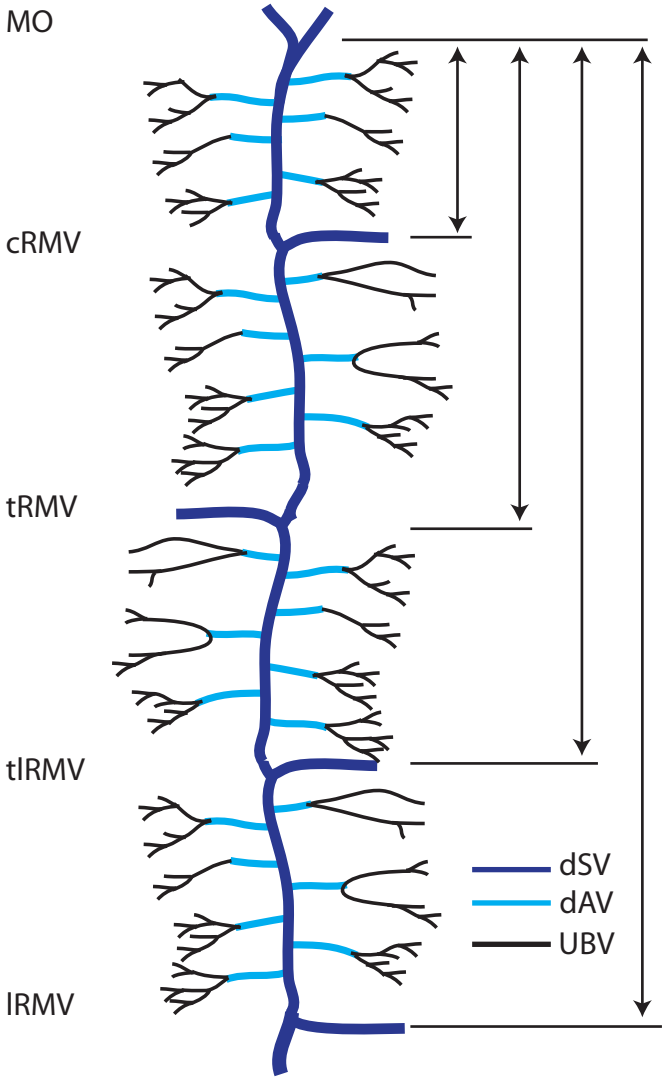

Supplementary Figure 1: The dorsal spinal vein (dSV) is characterized by at least four major radiculomadullary veins (RMVs) with a stereotyped spacing. We determined that the dSV in the C57B6/J mouse was drained along its length by four RMVs, occurring at the cervical level (cRMV), the mid-thoracic level (tRMV), thoracolumbar level (tlRMV), and the lumbar level (lRMV). The location of RMVs was measured from the bifurcation in the dSV at the medulla oblongata (MO) as shown by the dimension lines and found to be 5.1 ± 2 mm, 22.3 ± 7 mm, 34.5 ± 10 mm, and 47.4 ± 4 mm for the cRMV, tRMV, tlRMV and lRMV, respectively (n = 3 mice). Along its full length, the dSV is supplied by dorsal ascending venules (dAVs), which are in turn supplied by upstream branching venules (UBVs).

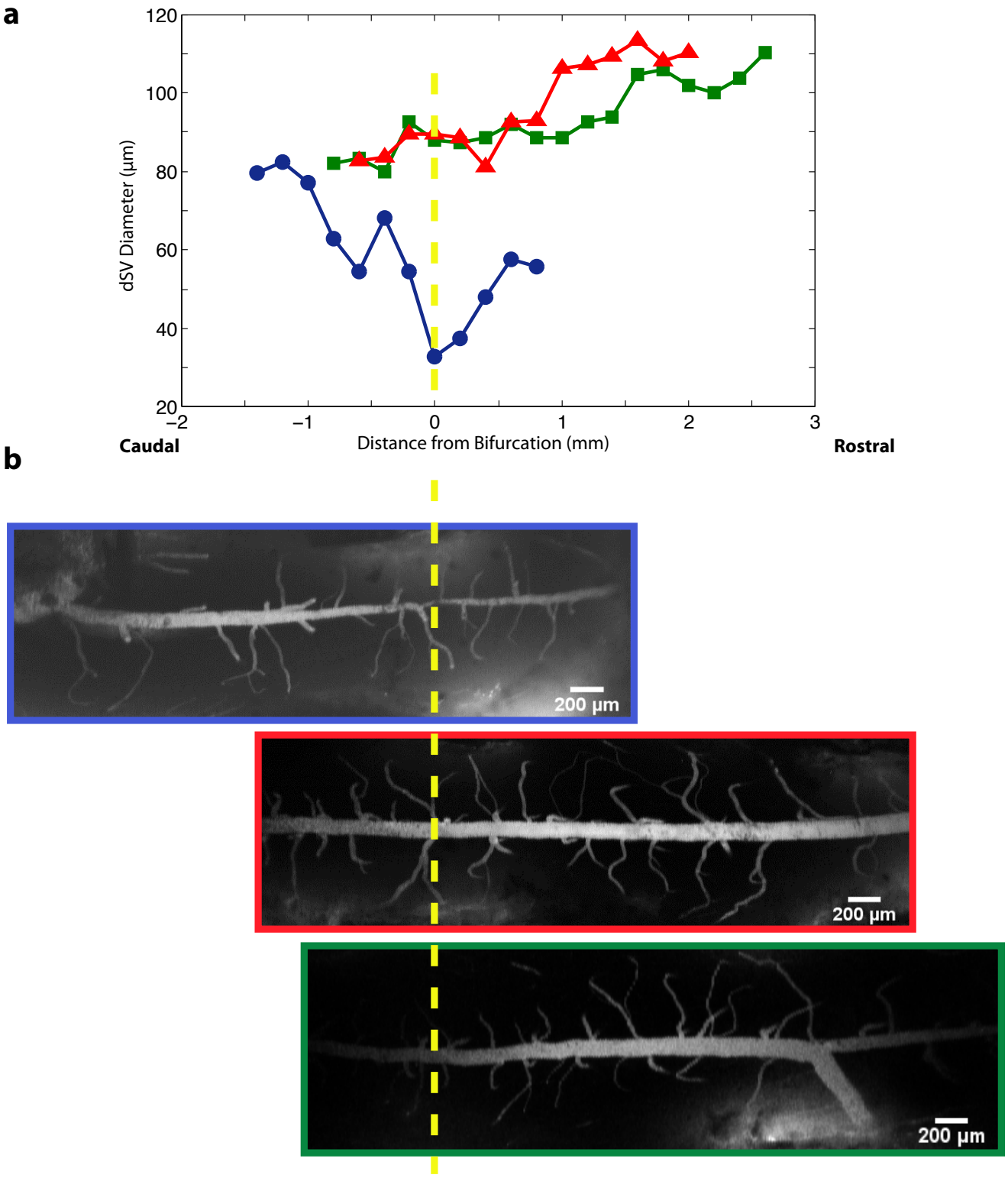

Supplementary Figure 2: The bifurcation in blood flow in the dSV is not reliably marked by a change in morphology. Diameter measurements of the dSV were made on either side of an observed bifurcation point (BP) (a). In one case (*blue line*), there was a significant decrease of the dSV diameter near the BP followed by a bilateral recovery of dSV diameter. 2PEF images taken of a large section of the dSV between branches (b) are shown for three mice. The dashed yellow line marks the BP in both the graph and images.

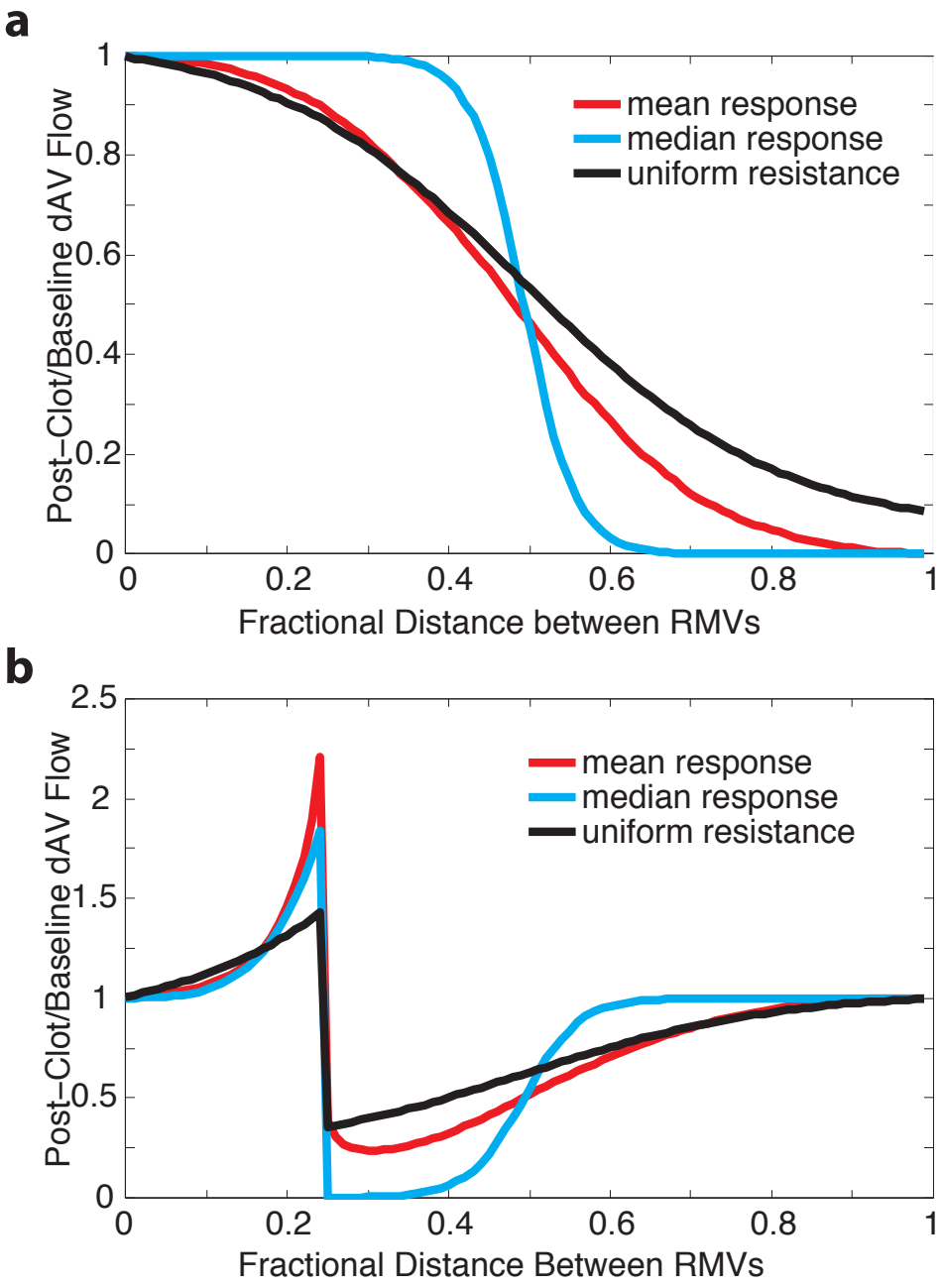

Supplementary Figure 3: Non-uniform resistance models of dorsal SCBF predict qualitatively similar results to a uniform-resistance model. We performed 1000 simulations of dorsal SCBF using variable resistances for clots at the rostral shunt (a) and at a fractional distance of 0.25 (b), corresponding to the approximate locations of our clotting experiments. The mean response (*red*) and median response (*cyan*) to simulated clots is shown in comparison to the uniform resistance model (*black*). The major source of variation owes to the variability in the location of the bifurcation, whose position shifts readily with asymmetries between the rostral (fractional distance > 0.5) and caudal (fractional distance < 0.5) ends of the dSV.